Guo *et al. Miner Miner Mater* 2024;3:6
DOI: 10.20517/mmm.2024.05

Minerals and Mineral Materials

Research Article

Open Access

Hectorite aerogel stabilized NaCl solution as composite phase change materials for subzero cold energy storage

Qijing Guo[1,2], Cong Guo[1,2], Ruishuang Zhang[2], Fangke Qin[2], Kai Zhao[2], Hao Yi[1,2]

[1]Key Laboratory of Green Utilization of Critical Non-metallic Mineral Resources, Ministry of Education, Wuhan University of Technology, Wuhan 430070, Hubei, China.
[2]School of Resources and Environmental Engineering, Wuhan University of Technology, Wuhan 430070, Hubei, China.

Correspondence to: Prof. Hao Yi, School of Resources and Environmental Engineering, Wuhan University of Technology, 122 Luoshi Road, Wuhan 430070, Hubei, China. E-mail: yihao287@whut.edu.cn

How to cite this article: Guo Q, Guo C, Zhang R, Qin F, Zhao K, Yi H. Hectorite aerogel stabilized NaCl solution as composite phase change materials for subzero cold energy storage. *Miner Miner Mater* 2024;3:6. https://dx.doi.org/10.20517/mmm.2024.05

Received: 8 Jan 2024 **First Decision:** 26 Mar 2024 **Revised:** 23 Apr 2024 **Accepted:** 29 Apr 2024 **Published:** 30 Apr 2024

Academic Editor: Hyunjung Kim **Copy Editor:** Dong-Li Li **Production Editor:** Dong-Li Li

Abstract

Inorganic phase change cold storage materials have garnered significant interest in cold chain transportation due to their high energy storage density. Nevertheless, practical applications have been hindered by inherent limitations such as high supercooling and susceptibility to phase separation. To address these challenges, this study devised 3D-Hectorite/sodium chloride (NaCl) composite phase change cold storage materials by utilizing 3D-Hectorite aerogel to adsorb NaCl solution, effectively mitigating the issue of phase separation common in such materials. Additionally, various concentrations of nucleating agents such as $SrCl_2 \cdot 6H_2O$, borax, and diatomite were introduced for step cooling curve tests, establishing 0.03% diatomite as the optimal concentration for nucleation, reducing the supercooling of the NaCl solution to 1.1 °C. The results showed that the latent heat and thermal conductivity of 3D-Hectorite/NaCl were 215.30 J/g and 0.6315 ± 0.013 W/mK, respectively. The phase transition temperature could be adjusted in the range of -33-0 °C by changing the concentration of NaCl to meet the different temperature requirements. Furthermore, exceptional cyclic stability was observed even after subjecting the material to ten dissolution-solidification cycles. Analyzing the temperature change of the air inside the insulation bag showed that, compared with ice, 3D-Hectorite/NaCl can be applied to meet lower cooling temperature requirements, demonstrating good prospects for its application in cold chain transportation.

Keywords: Phase change cold storage material, phase change temperature adjustable, sodium chloride, 3D-Aerogel, hectorite

INTRODUCTION

Phase change cold storage materials can store cold energy through the phase change process and release it when needed, offering an effective solution to the temporal and spatial mismatch of cold energy[1]. Due to their high energy storage density, they have found widespread application in various domains such as energy-efficient air conditioning[2,3], cold chain transportation[4,5], battery thermal management[6], and peak cut[7]. As living standards rise, there is a growing demand for fresh food items such as fruits, vegetables, fresh meats, and seafood. Cold chain transportation, serving as the principal means of transporting perishable foodstuffs, has garnered significant global attention. The traditional mechanical refrigeration systems have the problem of temperature fluctuation during transport, accompanied by a large amount of energy consumption and high carbon emissions[8]. In contrast, phase change cold storage materials are expected to make up for the shortcomings of traditional cold chain logistics due to their high energy storage density, good stability and reusability, which will help to improve the safety of food transported in the cold chain and reduce energy consumption.

In cold chain transport, selecting suitable phase change cold storage materials is crucial. Excellent phase change cold storage materials must exhibit high latent heat capacity, adjustable transition temperatures, excellent cyclic stability, and cost-effectiveness. At present, widely used phase change materials include organic and inorganic classifications[9]. Organic phase change cold storage materials, such as paraffin, fatty acids, and binary or ternary organic systems, offer distinct advantages, including high latent heat capacity, no supercooling, and chemical stability[10-12]. For instance, Zhang *et al.* devised a ternary organic phase change material comprising tetradecane, decanoic acid, and dodecanol, demonstrating a latent heat of 258.3 J/g, a transition temperature of 1.1 °C, and a thermal conductivity of 0.201 W/mK[13]. Similarly, Liu *et al.* formulated a glycine-based phase change material that significantly reduced pre-cooling time and the average temperature in refrigerated boxes by 68.4% and 2.55 °C, respectively[14]. Additionally, Liu *et al.* presented eutectic phase change materials of decanol and lauric acid with a phase change temperature of 2.8 °C and an enthalpy of 199.90 J/g, which showed good cycling stability[15]. Nevertheless, organic phase change cold storage materials still have defects, such as high cost, poor thermal conductivity, and flammability. In contrast, inorganic options for cold storage, such as water and hydrated salt, have the advantages of high latent heat, superior thermal conductivity, minimal volume change during phase transition, and cost-effectiveness. Water, one of the earliest and most widely used phase change materials, features a transition temperature of 0 °C and a latent heat of 334 J/g, boasting properties such as accessibility, cost-efficiency, and environmental friendliness. However, its transition temperature falls short of meeting the temperature requirements for storing and transporting frozen products. Studies have demonstrated that phase change cold storage materials with adjustable phase change temperatures can be prepared by adding dissolved salts to water to meet different cold chain temperature demands. For example, Xing *et al.* successfully lowered the transition temperature of water to -23.6 °C by introducing sodium formate and potassium chloride, rendering it suitable for storing and transporting frozen food items[16]. Likewise, Xu and Zhang reduced the phase transition temperature of water to -2.5 °C by adding a certain concentration of potassium sorbate[17].

However, the majority of inorganic phase change materials encounter challenges such as supercooling and phase separation during the transition process, necessitating the addition of suitable nucleating agents, thickeners, and supporting materials to enhance their performance[18-20]. Lin *et al.* effectively mitigated the phase separation and supercooling of decahydrate sodium sulfate by introducing carboxymethyl cellulose and borax, resulting in a reduction of the supercooling degree to 0.7 °C in the fabricated composite

material[21]. Additionally, Li *et al.* employed sodium polyacrylate as a thickener for eutectic hydrated salts, leading to the development of a phase change cold storage gel with a phase transition temperature of 7.71 °C and a latent heat of 122.1 J/g, exhibiting favorable cyclic stability[22]. Xing *et al.* utilized nano TiO_2 as a nucleating agent to minimize supercooling to 2.6 °C while effectively preventing phase separation and leakage by incorporating xanthan gum as a gelling agent[16]. Lin *et al.* innovatively utilized porous expanded graphite as a supporting material, thereby enhancing the shape stability and thermal conductivity of the phase change cold storage material, resulting in a 1.75-fold increase in its thermal conductivity[23]. Therefore, screening suitable nucleating agents and designing ideal porous support materials will significantly bolster the durability, thermal conductivity, and structural stability of composite phase change cold storage materials. Hectorite is a clay mineral containing magnesium, lithium, and silicon, with a trioctahedral crystal structure. It has exceptional gelling properties within aqueous systems and excellent thixotropy, dispersion, and thickening properties. Hectorite can rapidly swell in water to form a gel with extensive water network structures[24]. Our previous study has demonstrated that hectorite aerogels have a rich porous structure that can provide sufficient storage space for phase change thermal storage materials[25]. If hectorite aerogel is used as a supporting material to encapsulate inorganic salt solutions, a composite phase change cold storage material with stable structure and no phase separation can be obtained.

This study employs sodium chloride (NaCl) solution as a cold storage medium and aims to develop a novel 3D-Hectorite/NaCl composite phase change cold storage material, exhibiting adjustable phase change temperature, high latent heat, and stable cycling performance. Initially, the influence of nucleating agents, such as $SrCl_2·6H_2O$, diatomite, and borax, on the supercooling of NaCl solution was investigated. Subsequently, the modified NaCl solution is adsorbed into Hectorite aerogel to address phase separation issues. Furthermore, the impact of NaCl solution concentration on the phase change temperature of 3D-Hectorite/NaCl is explored. The synthesis mechanism, phase change performance, thermal conductivity, cycling stability, and cooling efficiency of 3D-Hectorite/NaCl are comprehensively examined to assess its potential application within the domain of cold chain logistics.

EXPERIMENTAL SECTION

Materials

NaCl, borax ($Na_2B_4O_7·10H_2O$), acetic acid (CH_3COOH), and diatomite were purchased from Sinopharm Chemical Reagent Co., Ltd., analytically pure. Glutaraldehyde (25% aqueous solution, $C_5H_8O_2$) and chitosan [$(C_6H_{11}NO_4)_n$] were purchased from Sinopharm Chemical Reagent Co., Ltd., biochemical reagents. Strontium chloride hexahydrate ($SrCl_2·6H_2O$) was purchased from Shanghai Aladdin Co., Ltd., analytically pure. Hectorite was provided by Hemings Advanced Materials Technology.

Preparation of 3D-Hectorite/NaCl

Preparation of 3D-Hectorite: At room temperature, chitosan (3 g) was added to 1% acetic acid solution (100 mL) and stirred for 30 min; then, hectorite (2 g) was added and stirred continuously for 1 h until uniform dispersion was achieved. Glutaraldehyde (1 mL) was added and stirred for 3 min to cross-link chitosan, and the resulting mixture was placed in the refrigerator. The frozen sample was dried in a vacuum freeze dryer (model: LGJ-12) for 48 h to obtain a 3D-hectorite aerogel.

Preparation of 3D-Hectorite/NaCl: 3D-Hectorite aerogel was immersed in 5 wt%, 10 wt%, and 15 wt% NaCl solutions for 10 min until saturated, resulting in the production of three distinct 3D-Hectorite/NaCl composite phase change cold storage materials, designated as 3D-Hectorite/NaCl-5, 3D-Hectorite/NaCl-10, and 3D-Hectorite/NaCl-15. In addition, taking 3D-Hectorite/NaCl-5 as an example, different nucleating agents ($SrCl_2·6H_2O$, borax, diatomite) were added to 5 wt% NaCl solution to regulate the supercooling inhibition of composite phase change cold storage materials.

Characterization

The microstructure of the sample was characterized by scanning electron microscopy (SEM, Phenom ProX). The functional groups of the sample were observed using a Fourier transform infrared spectrometer (FTIR, Nicolet 6700), with a wavenumber range of 4,000-400 cm^{-1}. Differential scanning calorimetry (DSC25) was employed to analyze the thermal properties of the sample, including phase transition temperature and latent heat. The thermal conductivity of the sample at 25 °C was measured using a thermal conductivity meter (Hot Disk, TPS 2500S), and the measurement results were the average of three results. The step cooling curve and supercooling degree of the samples were determined using the temperature probe of Elitech GSP-6 smart thermometer to collect the temperature data inside the composite phase change storage material.

RESULTS AND DISCUSSION

Microstructure and synthetic mechanism

The micrographs [Figure 1A and B], images [Figure 1C], and optical microscopy image [Figure 1D] of the 3D-Hectorite aerogels delineate their rich micron-scale porous architecture. This structure enables the adsorption and retention of phase-change cold-storage materials through capillary action. The notably high porosity inherent in these aerogels confers substantial storage capacity for these materials. The aerogel, after adsorption of the cold storage material [Figure 1E and F], and the NaCl solution is fully filled in the pore structure of the 3D-Hectorite aerogel. The porous structure of the aerogel provides a barrier for the NaCl solution, which can effectively prevent the leakage problem of the composite phase change cold storage materials.

Figure 2A shows the FTIR spectra of hectorite, chitosan and 3D-Hectorite aerogel. In the FTIR spectra of hectorite, the strong and broad absorption bands appearing at 3,456 cm^{-1} are caused by structural hydroxyl groups and hydroxyl group vibrations in interlayer water[26]. The peak at 1,639 cm^{-1} corresponds to the bending vibration of H-OH, while the peak at 1,009 cm^{-1} corresponds to the stretching vibration of Si-O and Si-O-Si[25,27]. The peaks at 653 and 447 cm^{-1} correspond to OH bending vibrations caused by adsorbed water and Mg-O stretching vibrations, respectively[28]. In the FTIR spectrum of chitosan, the peak at 3,374 cm^{-1} corresponds to the overlap of O-H and N-H stretching vibrations and hydrogen bonding between chitosan chains[29,30]. The peaks at 2,877 and 1,422 cm^{-1} are attributed to the vibrations of pyranose rings, assigned to CH_2 stretching and OH/CH vibrations, respectively[31]. The peaks at 1,657 and 1,560 cm^{-1} are due to the C=O bending vibration of the -NHCO- group (amide I) and the N-H stretching vibration of the $-NH_2$ group (amide II), respectively[32,33]. The absorption band around 1,031 cm^{-1} is attributed to the stretching vibration of the C-O-C group in the glycosidic bond[34]. In the FTIR spectrum of 3D-Hectorite, all characteristic peaks correspond to hectorite and chitosan, and no new peaks are generated, indicating that the materials are only physically combined without undergoing any chemical reactions. Specifically, the O-H and N-H stretching vibrations at 3,374 cm^{-1} of chitosan coincide with the hydroxyl vibration of hectorite at 3,456 cm^{-1} at 3,412 cm^{-1}, which is related to the hydrogen bonding between chitosan and hectorite[35]. These results unequivocally suggest that the binding of 3D-Hectorite is exclusively facilitated by physical interactions, devoid of any chemical reactivity. The preparation process and cross-linking mechanism of 3D-Hectorite are shown in Figure 2B. There are various physical interactions in the aerogel network; for example, the exposed hydroxyl groups on the hectorite surface can form hydrogen bonds with -OH groups on the chitosan chains, between the chains of chitosan molecules, and between the hectorite nanosheets. Additionally, the negative charge present on the surface of hectorite can engage in electrostatic interactions with $-NH_2$ groups on the chitosan chain.

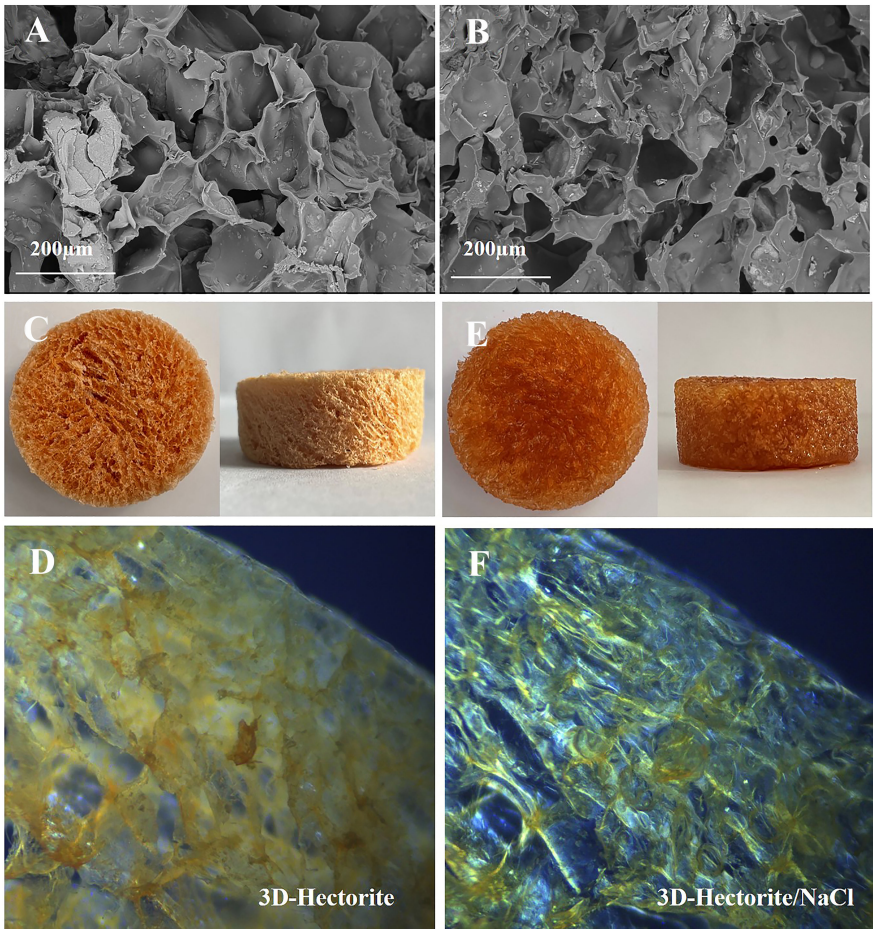

Figure 1. (A and B) SEM images; (C) Top view and side view of 3D-hectorite; (D) Top view and side view of 3D-Hectorite/NaCl; Optical microscopy images of (E) 3D-hectorite aerogel and (F) 3D-Hectorite/NaCl. SEM: Scanning electron microscopy.

Supercooling suppression regulation

The problem of supercooling is not conducive to the timely release of latent heat, which largely limits the further development of inorganic salt phase change materials. Based on the heterogeneous nucleation theory, the supercooling of NaCl solution is regulated by adding nucleating agents. In the preparation of composite phase change cold storage materials, taking 5 wt% NaCl solution as an example, the inhibitory effect of nucleating agents ($SrCl_2·6H_2O$, borax, diatomite) on the supercooling of NaCl was investigated, and the supercooling under different nucleating agent doping amounts was analyzed. The composition ratios of the samples are shown in Table 1. The results can provide insights into optimizing the preparation process of composite phase change materials with enhanced cold storage properties.

When utilizing $SrCl_2·6H_2O$ as a nucleating agent, the corresponding step cooling curves and degrees of supercooling are depicted in Figure 3A and B. The supercooling of the NaCl solution, without the addition of $SrCl_2·6H_2O$, measures at 6.8 °C. Upon introducing 0.5 wt% $SrCl_2·6H_2O$, it diminishes to 2.6 °C. However, with escalating concentrations of $SrCl_2·6H_2O$ to 1.0 wt% and 1.5 wt%, it subsequently escalates to 3.9 and 5.1 °C, respectively. Analysis of the step cooling curves indicates that its effective reduction following the inclusion of $SrCl_2·6H_2O$. Adding 0.5 wt% $SrCl_2·6H_2O$ yields the most significant reduction in supercooling for the NaCl solution. Nonetheless, as the quantity of $SrCl_2·6H_2O$ increases, it exhibits a gradual upward trend. Furthermore, when employing Borax as the nucleating agent, its corresponding step cooling curves

Table 1. Sample composition ratios

Sequence	NaCl	Nucleating agents	H_2O
1	5 wt%	0 wt%	95 wt%
2	5 wt%	0.5 wt% $SrCl_2·6H_2O$	94.5 wt%
3	5 wt%	1 wt% $SrCl_2·6H_2O$	94 wt%
4	5 wt%	1.5 wt% $SrCl_2·6H_2O$	93.5 wt%
5	5 wt%	0.5 wt% borax	94.5 wt%
6	5 wt%	1.0 wt% borax	94 wt%
7	5 wt%	1.5 wt% borax	93.5 wt%
8	5 wt%	0.01 wt% diatomite	94.99 wt%
9	5 wt%	0.02 wt% diatomite	94.98 wt%
10	5 wt%	0.03 wt% diatomite	94.97 wt%

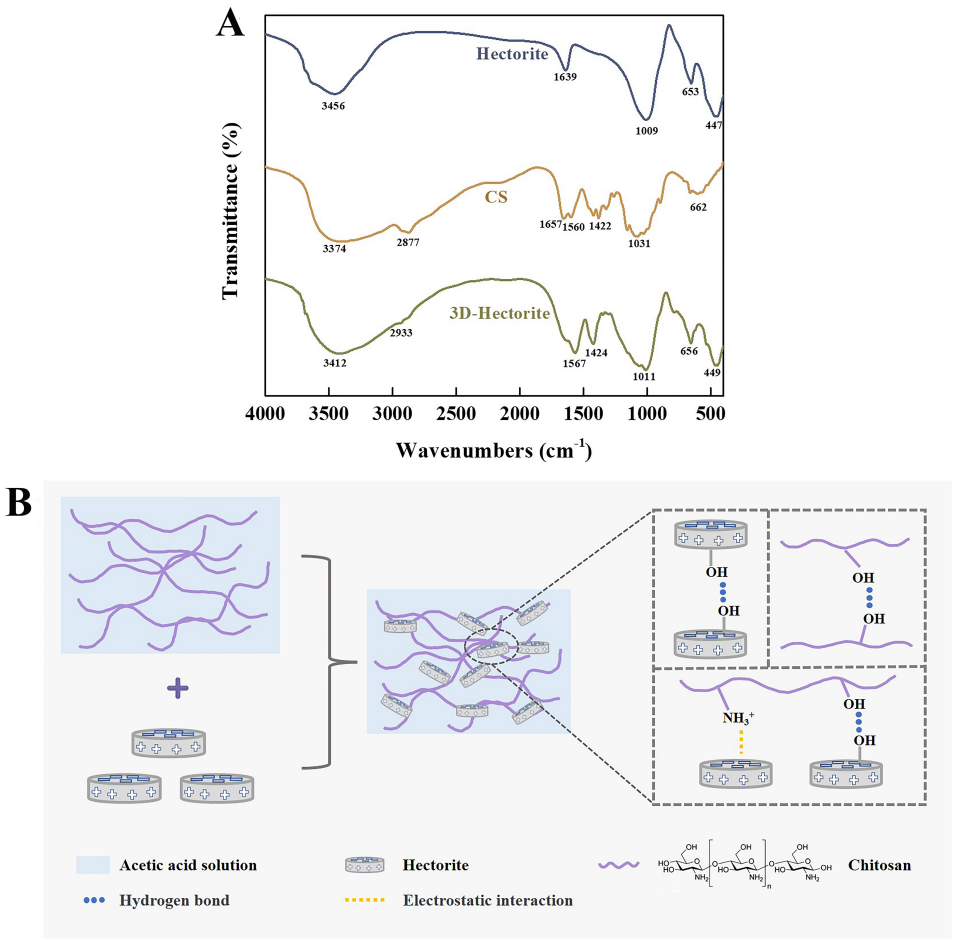

Figure 2. (A) FTIR spectra of hectorite, chitosan and 3D-Hectorite aerogel; (B) The preparation process and cross-linking mechanism of 3D-Hectorite. FTIR: Fourier transform infrared spectrometer.

and degrees are illustrated in Figure 3C and D. Supercooling diminishes to 3.0 and 1.7 °C with Borax additions of 0.5 wt% and 1.0 wt%, respectively. However, with an increase in the dosage to 1.5 wt%, it subsequently rises to 3.9 °C. The trend in supercooling variation is similar to that observed when $SrCl_2·6H_2O$ is added. The main reasons for these results are[36]: (1) The nucleating agents provide a large

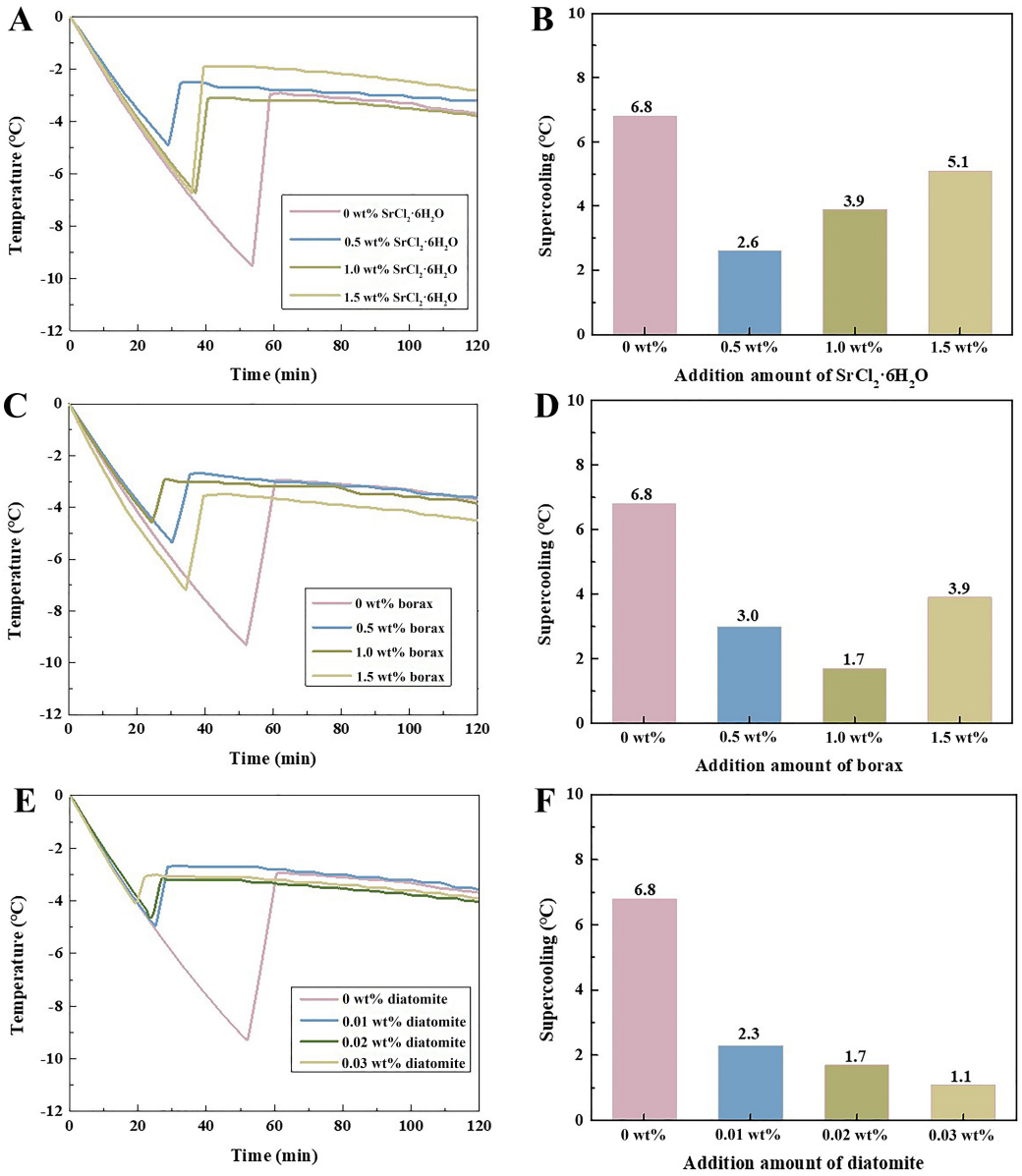

Figure 3. Step cooling curves of 5 wt% NaCl solution with different amounts of (A) $SrCl_2·6H_2O$, (C) borax, (E) diatomite; Supercooling degree of 5 wt% NaCl solution with different amounts of (B) $SrCl_2·6H_2O$, (D) borax, (F) diatomite.

number of nucleation sites, reducing the supercooling degree by lowering the energy potential barrier for material nucleation; (2) When the quantity of nucleating agents increases, part will be deposited on the phase change material, inhibiting the combination of salt and water in the solution; (3) The growth of nuclei is influenced by the force of nucleating atoms, which escalates with increasing nucleating agent content and further inhibits their growth; (4) The surface free energy of nucleation elevates with rising nucleating agent content, which can hinder the nucleation formation to a certain extent, thereby augmenting the degree of supercooling. In addition, the effect of diatomite as a nucleating agent on the supercooling degree of NaCl solution was explored. The supercooling degrees of NaCl solutions were 6.8, 2.3, 1.7 and 1.1 °C when diatomite was added at 0 wt%, 0.01 wt%, 0.02 wt% and 0.03 wt%, respectively [Figure 3E and F]. Following a comprehensive comparison of the supercooling inhibition effects of the three nucleating agents, diatomite

was selected as the subsequent experimental nucleating agent, with a controlled addition rate set at 0.03 wt%.

Phase change characteristics

Utilizing diatomite as the nucleating agent, three distinct 3D-Hectorite/NaCl composite phase change cold storage materials were synthesized using 5 wt%, 10 wt%, and 15 wt% NaCl solutions, denoted as 3D-Hectorite/NaCl-5, 3D-Hectorite/NaCl-10, and 3D-Hectorite/NaCl-15, respectively. Differential scanning calorimetry (DSC) tests were conducted on these materials to investigate the influence of NaCl solution concentration on sample phase transition temperatures and latent heats. Figure 4 illustrates the DSC curves of the three composite phase change cold storage materials, and the corresponding phase change temperatures and latent heats are summarized in Table 2. The melting latent heats of 3D-Hectorite/NaCl-5, 3D-Hectorite/NaCl-10, and 3D-Hectorite/NaCl-15 were respectively measured at 212.78, 201.45, and 215.30 J/g, while their solidification latent heats were recorded as 193.71, 198.62, and 186.90 J/g, all exhibiting a decrease with increasing NaCl solution concentration. Additionally, the melting temperatures of 3D-Hectorite/NaCl-5, 3D-Hectorite/NaCl-10, and 3D-Hectorite/NaCl-15 were observed at -4.42, -8.76, and -19.55 °C, respectively, with their corresponding solidification temperatures at -14.61, -22.32, and -33.99 °C, showcasing a gradual decrease trend. The results indicate that the 3D-Hectorite/NaCl composite phase change cold storage materials possess suitable low-temperature phase transition temperatures and high latent heat values, and the phase transition temperatures can be adjusted as needed by changing the NaCl solution concentration, showing practical application potential.

Thermal conductivity

The thermal conductivity of composite phase change materials crucially influences their energy storage and release efficiency. The transient plane heat source method was used to measure the thermal conductivity of 3D-Hectorite/NaCl-5, 3D-Hectorite/NaCl-10, and 3D-Hectorite/NaCl-15 at room temperature (25 °C), which were found to be 0.6606 ± 0.033, 0.6190 ± 0.027, and 0.6315 ± 0.013 W/mK, respectively, indicating comparable thermal performance. The results show that the thermal conductivity of 3D-Hectorite/NaCl composite phase change cold storage materials remains unaffected by variations in NaCl solution concentration. Furthermore [Table 3], compared to other phase change cold storage materials (especially organic phase change materials), the 3D-Hectorite/NaCl prepared in this study exhibits excellent thermal conductivity, ensuring efficient energy storage and release.

Cycle performance

In practical applications, the longevity of phase change cold storage materials hinges upon the stability of their thermophysical properties. We conducted 100 solidification-melting cycles on 3D-Hectorite/NaCl-15 (samples were frozen in liquid nitrogen and thawed at room temperature), and the samples were tested for DSC and thermal conductivity before and after the cycles. As depicted in Figure 5A-D, the melting temperatures of 3D-Hectorite/NaCl-15 for the 1st, 10th, and 100th cycles were recorded as -19.55, -19.70, and -19.52 °C, respectively, with corresponding melting enthalpies of 215.30, 207.60, and 181.87 J/g; while the solidification temperatures were -33.99, -30.04, and -34.56 °C, respectively, with corresponding solidification enthalpies of 186.90, 180.33, and 164.80 J/g. The melting enthalpy of 3D-Hectorite/NaCl-15 decreased by 3.58% and 15.53% after ten and 100 cycles, respectively, while the corresponding solidification enthalpy decreased by 3.52% and 11.82%, respectively. The results indicate that the thermophysical properties of this composite phase change material fluctuate less before and after cycling and show good cycling stability.

Cold storage application effect

The evaluation of practical application potential was conducted by assessing the latent cold storage effect of

Table 2. Thermal properties of 3D-Hectorite/NaCl composites

Sample	Freezing temperature (°C)	Freezing latent heat (J/g)	Melting temperature (°C)	Melting latent heat (J/g)
3D-Hectorite/NaCl-5	-14.61	193.71	-4.42	212.78
3D-Hectorite/NaCl-10	-22.32	198.62	-8.76	201.45
3D-Hectorite/NaCl-15	-33.99	186.9	-19.55	215.30

Table 3. Comparison of thermal conductivity of the 3D-Hectorite/NaCl composites with other PCMs

Sample	Thermal conductivity (W/mK)	Ref.
SSD-BCKN3	0.264	[21]
Tetradecane-lauryl alcohol	0.2737	[37]
Oleic-myristic acid	0.2513	[38]
Ag-doped ZnO-oleic acid-myristic acid eutectic PCM mixtures	0.3735	
Lauryl alcohol-Capric acid/CuO	0.174	[39]
Brine phase change material gel (NH_4Cl/KCl/H_2O)	0.589	[40]
Mannitol/$MgCl_2$@MWCNT-OH/PAM	0.685	[41]
PEG400/Terminalia catappa	0.411	[42]
3D-Hectorite/NaCl-5	0.6606	This work
3D-Hectorite/NaCl-10	0.6190	
3D-Hectorite/NaCl-15	0.6315	

PCMs: Phase change materials.

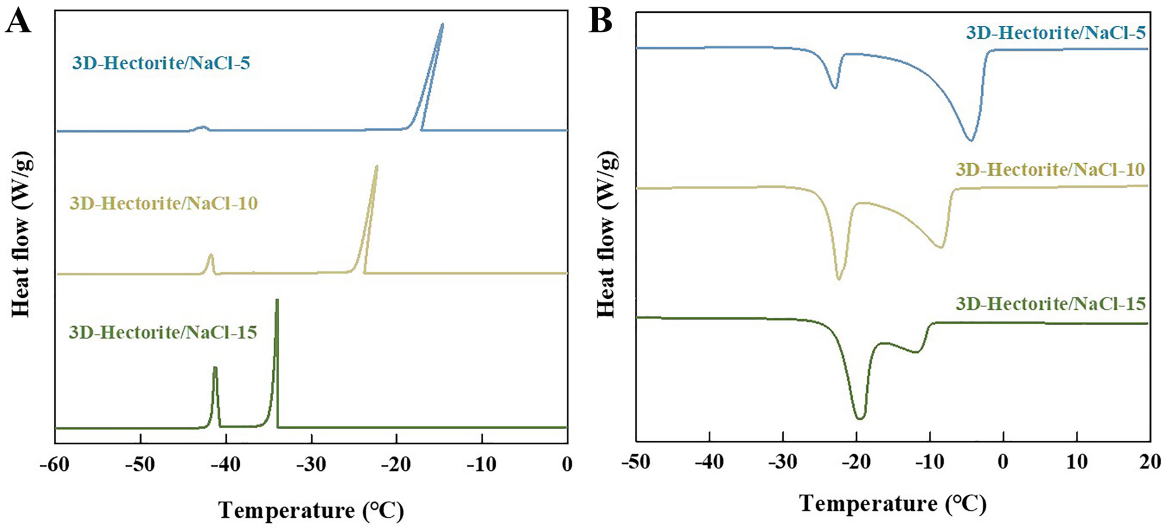

Figure 4. (A) Cooling and (B) melting DSC curves of 3D-Hectorite/NaCl composites. DSC: Differential scanning calorimetry.

the test samples. As shown in Figure 6A, the insulation bag in this test features a triangular prism structure. In the cold storage test, the sample was prepared into three rectangular structures with the same dimensions as the side walls of the thermal insulation bag. The frozen sample was placed in a sealed bag positioned close to the side wall of the insulation bag, with a partition used to separate the sample from the internal environment of the bag. Equal amounts (controlled at 100 g) of frozen water, 3D-Hectorite/NaCl-5, 3D-Hectorite/NaCl-10 and 3D-Hectorite/NaCl-15 were positioned snugly against the sidewalls of the insulation

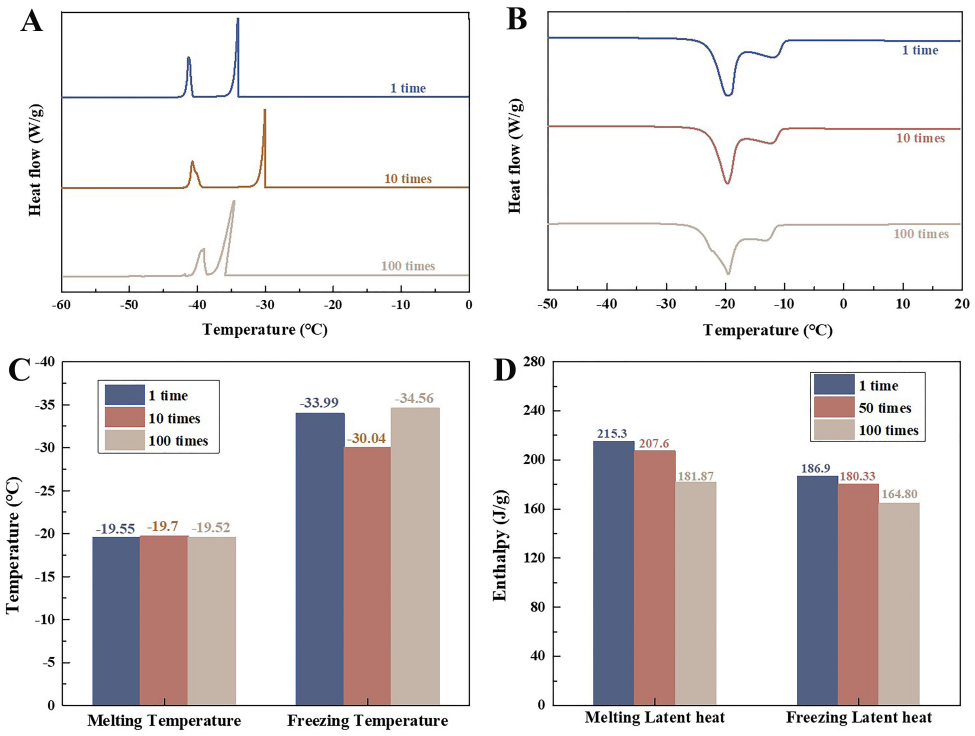

Figure 5. (A) Cooling and (B) melting DSC curves, (C) phase transition enthalpy and (D) peak phase transition temperature of 3D-Hectorite/NaCl-15 before and after cycling. DSC: Differential scanning calorimetry.

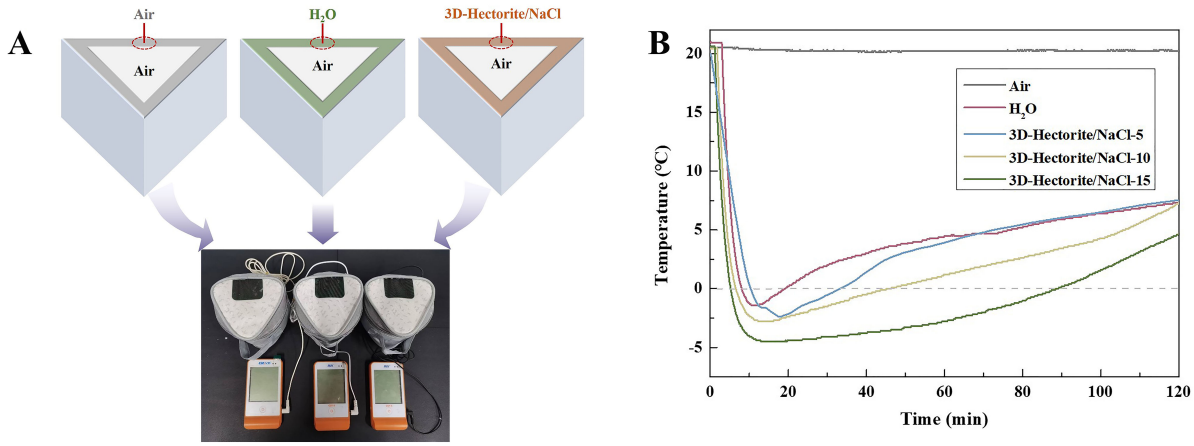

Figure 6. (A) Cold storage test unit; (B) Curve of the cooling effect of 3D-Hectorite/NaCl.

bags. Temperature probes were employed to monitor variations in the air temperature at the center of the insulation bags, with an empty insulation bag as the blank control group. The ambient temperature during testing was approximately 22 °C, while the initial temperature inside the insulation bag was maintained at 21 ± 1 °C. The results depicted in Figure 6B revealed that the average temperature of the control group remained constant at 20.7 °C. Within the insulation bag utilizing water as the cold storage medium, the air temperature could reach a minimum of -1.4 °C but sustained subzero temperatures for only approximately ten minutes. However, using 3D-Hectorite/NaCl-5, 3D-Hectorite/NaCl-10, and 3D-Hectorite/NaCl-15

lowered the air temperatures within the insulation bags to -2.3, -2.8, and -4.5 °C, respectively, sustaining subzero temperatures for 24, 40, and 85 min, respectively. These results indicate that 3D-Hectorite/NaCl enables the insulation bags to sustain a prolonged subzero temperature state. This is attributed to the lower phase transition temperature of 3D-Hectorite/NaCl. Frozen 3D-Hectorite/NaCl can melt at more negative temperatures, thereby reducing the ambient temperature inside the bag and maintaining subzero levels. Moreover, as NaCl concentration increases, the duration of subzero temperature maintenance is extended. However, ice undergoes phase transition near 0 °C, limiting its ability to lower the temperature inside the bag to around zero degrees and maintain a subzero cryogenic state for a short period. This observation underscores the significant potential of this technology for applications in cold chain transport.

CONCLUSIONS

In this study, three nucleating agents, including $SrCl_2·6H_2O$, borax, and diatomite, were screened to identify the most effective type and dosage for reducing the supercooling of NaCl solution. On this basis, employing 3D-Hectorite aerogel as a supporting material, NaCl solution was adsorbed, resulting in the fabrication of a shape-stable 3D-Hectorite/NaCl composite phase change material. The developed 3D-Hectorite/NaCl material exhibited impressive melting and solidification enthalpies of 215.30 and 186.9 J/g, respectively, while maintaining stable thermophysical properties before and after the melting-solidification cycles. Additionally, the material demonstrated adjustable phase change temperatures, rendering it adaptable to a wide range of temperature requirements. In summary, the synthesized 3D-Hectorite/NaCl presents an effective solution for mitigating supercooling and phase separation, offering promising prospects for application in cold chain transportation within the foreseeable future.

DECLARATIONS

Author' contributions

Conceptualization, methodology, investigation, writing - original draft preparation, writing-reviewing and editing: Guo Q

Methodology, investigation: Guo C, Zhang R, Qin F, Zhao K
Resources, supervision, writing-reviewing and editing: Yi H

Availability of data and materials

Not applicable.

Financial support and sponsorship

This work was supported by the National Natural Science Foundation of China (52104265) and National Innovation and Entrepreneurship Training Program for College Students (S202310497274).

Conflict of interest

Yi H is an Editorial Board member of the journal *Minerals and Mineral Materials*, while the other authors have declared that they have no conflicts of interest.

Ethical approval and consent to participate

Not applicable.

Consent for publication

Not applicable.

REFERENCES

1. Zhang L, Xia X, Lv Y, et al. Fundamental studies and emerging applications of phase change materials for cold storage in China. *J Energy Storage* 2023;72:108279. DOI
2. Shao J, Darkwa J, Kokogiannakis G. Development of a novel phase change material emulsion for cooling systems. *Renew Energy* 2016;87:509-16. DOI
3. Li S, Liu Z, Wang X. A comprehensive review on positive cold energy storage technologies and applications in air conditioning with phase change materials. *Appl Energy* 2019;255:113667. DOI
4. Soltani M, Chahartaghi M, Majid Hashemian S, Faghih Shojaei A. Technical and economic evaluations of combined cooling, heating and power (CCHP) system with gas engine in commercial cold storages. *Energy Convers Manag* 2020;214:112877. DOI
5. Meng B, Zhang X, Hua W, Liu L, Ma K. Development and application of phase change material in fresh e-commerce cold chain logistics: a review. *J Energy Storage* 2022;55:105373. DOI
6. Nie B, Palacios A, Zou B, Liu J, Zhang T, Li Y. Review on phase change materials for cold thermal energy storage applications. *Renew Sustain Energy Rev* 2020;134:110340. DOI
7. Uddin M, Romlie MF, Abdullah MF, Abd Halim S, Abu Bakar AH, Chia Kwang T. A review on peak load shaving strategies. *Renew Sustain Energy Rev* 2018;82:3323-32. DOI
8. Sha Y, Hua W, Cao H, Zhang X. Properties and encapsulation forms of phase change material and various types of cold storage box for cold chain logistics: a review. *J Energy Storage* 2022;55:105426. DOI
9. Mehrizi AA, Karimi-maleh H, Naddafi M, Karimi F. Application of bio-based phase change materials for effective heat management. *J Energy Storage* 2023;61:106859. DOI
10. Eanest Jebasingh B, Valan Arasu A. Characterisation and stability analysis of eutectic fatty acid as a low cost cold energy storage phase change material. *J Energy Storage* 2020;31:101708. DOI
11. Feng T, Ji J, Zhang X. Research progress of phase change cold energy storage materials used in cold chain logistics of aquatic products. *J Energy Storage* 2023;60:106568. DOI
12. Ma Y, Zou M, Chen W, et al. A structured phase change material integrated by MXene/AgNWs modified dual-network and polyethylene glycol for energy storage and thermal management. *Appl Energy* 2023;349:121658. DOI
13. Zhang G, Chen L, Lu W, Wu Z. Production of ternary organic phase change material combined with expanded graphite and its application in cold chain transportation. *Therm Sci Eng Prog* 2023;46:102204. DOI
14. Liu Y, Li M, Zhang Y, et al. Preparation and stability analysis of glycine water-based phase change materials modified with potassium sorbate for cold chain logistics. *J Energy Storage* 2023;72:108375. DOI
15. Liu L, Zhang X, Xu X, et al. Development of low-temperature eutectic phase change material with expanded graphite for vaccine cold chain logistics. *Renew Energy* 2021;179:2348-58. DOI
16. Xing X, Lu W, Zhang G, et al. Ternary composite phase change materials (PCMs) towards low phase separation and supercooling: eutectic behaviors and application. *Energy Rep* 2022;8:2646-55. DOI
17. Xu X, Zhang X. Simulation and experimental investigation of a multi-temperature insulation box with phase change materials for cold storage. *J Food Eng* 2021;292:110286. DOI
18. Zhao Y, Zhang X, Xu X, Zhang S. Research progress in nucleation and supercooling induced by phase change materials. *J Energy Storage* 2020;27:101156. DOI
19. Liu K, He Z, Luo Y, Lin P, Chen Y. Massive fabrication of flexible, form-stable, and self-repairing brine phase change material gels toward smart cold chain logistics. *ACS Appl Mater Interfaces* 2023;15:17091-102. DOI
20. Liu Y, Li M, Emam Hassanien RH, Wang Y, Tang R, Zhang Y. Fabrication of shape-stable glycine water-based phase-change material using modified expanded graphite for cold energy storage. *Energy* 2024;290:130306. DOI
21. Lin N, Li C, Zhang D, Li Y, Chen J. Emerging phase change cold storage materials derived from sodium sulfate decahydrate. *Energy* 2022;245:123294. DOI
22. Li C, Li Y, He Y. Optimization of super water-retention phase change gels for cold energy storage in cold chain transportation. *J Energy Storage* 2023;61:106719. DOI
23. Lin N, Li C, Zhang D, Li Y, Chen J. Enhanced cold storage performance of $Na_2SO_4 \cdot 10H_2O$/expanded graphite composite phase change materials. *Sustain Energy Technol Assess* 2021;48:101596. DOI
24. Zhang J, Zhou CH, Petit S, Zhang H. Hectorite: synthesis, modification, assembly and applications. *Appl Clay Sci* 2019;177:114-38. DOI
25. Guo Q, Yi H, Jia F, Song S. Vertical porous MoS_2/hectorite double-layered aerogel as superior salt resistant and highly efficient solar steam generators. *Renew Energy* 2022;194:68-79. DOI

26. Zeng J, Tong X, Ren P, Chen L. Theoretical description on size matching for magnetic element to independent particle in high gradient magnetic separation. *Miner Eng* 2019;135:74-82. DOI
27. Nair BP, Sindhu M, Nair PD. Polycaprolactone-laponite composite scaffold releasing strontium ranelate for bone tissue engineering applications. *Colloids Surf B Biointerfaces* 2016;143:423-30. DOI PubMed
28. Nabipour H, Wang X, Song L, Hu Y. Laponite-based inorganic-organic hybrid coating to reduce fire risk of flexible polyurethane foams. *Appl Clay Sci* 2020;189:105525. DOI
29. Wang W, Zhang C, He J, et al. Chitosan-induced self-assembly of montmorillonite nanosheets along the end-face for methylene blue removal from water. *Int J Biol Macromol* 2023;227:952-61. DOI
30. Chen P, Zeng S, Zhao Y, Kang S, Zhang T, Song S. Synthesis of unique-morphological hollow microspheres of MoS_2@ montmorillonite nanosheets for the enhancement of photocatalytic activity and cycle stability. *J Mater Sci Technol* 2020;41:88-97. DOI
31. Rakkapao N, Vao-soongnern V, Masubuchi Y, Watanabe H. Miscibility of chitosan/poly(ethylene oxide) blends and effect of doping alkali and alkali earth metal ions on chitosan/PEO interaction. *Polymer* 2011;52:2618-27. DOI
32. Kasinathan K, Murugesan B, Pandian N, Mahalingam S, Selvaraj B, Marimuthu K. Synthesis of biogenic chitosan-functionalized 2D layered MoS_2 hybrid nanocomposite and its performance in pharmaceutical applications: in-vitro antibacterial and anticancer activity. *Int J Biol Macromol* 2020;149:1019-33. DOI PubMed
33. Guo Q, An Q, Yi H, Jia F, Song S. Double-layered montmorillonite/MoS_2 aerogel with vertical channel for efficient and stable solar interfacial desalination. *Appl Clay Sci* 2022;217:106389. DOI
34. Morariu S, Brunchi CE, Honciuc M, Iftime MM. Development of hybrid materials based on chitosan, poly(ethylene glycol) and laponite® RD: effect of clay concentration. *Polymers* 2023;15:841. DOI PubMed PMC
35. Ranjbardamghani F, Eslahi N, Jahanmardi R. An injectable chitosan/laponite hydrogel synthesized via hybrid cross-linking system: a smart platform for cartilage regeneration. *Polym Adv Tech* 2023;34:2298-311. DOI
36. Zou T, Fu W, Liang X, et al. Preparation and performance of modified calcium chloride hexahydrate composite phase change material for air-conditioning cold storage. *Int J Refrig* 2018;95:175-81. DOI
37. Zhao Y, Zhang X, Xu X, Zhang S. Development of composite phase change cold storage material and its application in vaccine cold storage equipment. *J Energy Storage* 2020;30:101455. DOI
38. Dhivya S, Hussain SI, Jeya Sheela S, Kalaiselvam S. Experimental study on microcapsules of Ag doped ZnO nanomaterials enhanced Oleic-Myristic acid eutectic PCM for thermal energy storage. *Thermochim Acta* 2019;671:70-82. DOI
39. Sarafoji P, Mariappan V, Anish R, Karthikeyan K, Kalidoss P. Characterization and thermal properties of Lauryl alcohol - Capric acid with CuO and TiO_2 nanoparticles as phase change material for cold storage system. *Mater Lett* 2022;316:132052. DOI
40. Liu K, He Z, Lin P, et al. Highly-efficient cold energy storage enabled by brine phase change material gels towards smart cold chain logistics. *J Energy Storage* 2022;52:104828. DOI
41. Ma K, Zhang X, Ji J, Han L. Development, characterization and modification of mannitol-water based nanocomposite phase change materials for cold storage. *Colloids Surf A Physicochem Eng Asp* 2022;650:129571. DOI
42. Kumar P, Thomas S, Sobhan C, Peterson G. Activated carbon foam composite derived from PEG400/Terminalia Catappa as form stable PCM for sub-zero cold energy storage. *J Clean Prod* 2024;434:139993. DOI